

# I. HEAVY-ION NUCLEAR PHYSICS RESEARCH

## OVERVIEW

This research involves investigating the structure, stability, reactions and decays of nuclei. This information is crucial for understanding the evolution of the universe, the workings of stars and the abundances of the elements that form the world around us. The forefront area of research is investigating the properties of nuclei which lie very far from stability, and which are critical in understanding nucleosynthesis. Most of our research is based at the Argonne Tandem-Linac Accelerator (ATLAS), a national heavy-ion user facility. During this year programs were also mounted at the Relativistic Heavy Ion Collider (RHIC), at Michigan State University, at Yale University, and at other forefront facilities. The major thrusts of the program are: a) deepening and generalizing our understanding of nuclear structure to allow a reliable description of all bound nuclear systems, b) studying the reactions that are important in the cataclysmic events in the cosmos which lead to the synthesis of the chemical elements, c) testing the limits of the Standard Model, the fundamental theory that currently best represents our understanding of the laws and fundamental symmetries of nature.

The specific research topics we are pursuing include the measurements of reactions that are important in astrophysics. Many approaches are used, including the production and acceleration of short-lived nuclei in order to measure key reaction rates, and the use of Gammasphere to investigate the properties of states in the "Gamow window". A strong program of nuclear physics measurements on trapped atoms and ions is developing. An "online" atom trap now complements the existing CPT Penning ion trap and there is rapid development of a new "open-geometry" trap for weak interaction studies. The return of Gammasphere opens new opportunities for gamma-spectroscopy and a wide range of experiments are being carried out on both neutron-rich and neutron poor nuclei. The key thrust of spectroscopic studies is to investigate the modification of residual interactions in nuclei far from stability. In addition, there are complimentary efforts in the use of Accelerator Mass Spectrometry (AMS) for environmental research and in the investigation of nuclear matter at relativistic energies. The ATLAS-based research exploits the unique capabilities of the accelerator, both in the stable beam program, and in production of accelerated beams of short-lived isotopes. The experiments employ state-of-the-art research equipment, including the National Gamma Ray Facility Gammasphere, the Fragment Mass Analyzer (FMA), a large solid angle silicon array, "Ludwig", and the Canadian Penning Trap, (CPT) all of which are operating at ATLAS. Several new detector initiatives are being pursued including refining the "In-Flight" radioactive beam facility and its detector systems, constructing the Advanced Penning Trap (APT), and development of the online atom trap (ATTA). Considerable effort continues in developing the next generation gamma ray detectors with "tracking" capability, and development of a compact and efficient array for decay studies (the X-Array). Intensive participation in the PHOBOS experiment at Brookhaven has continued.

Some of the specific goals of the program can be summarized as follows:

- Develop and utilize beams of short-lived nuclei,  ${}^6\text{He}$ ,  ${}^8\text{Li}$ ,  ${}^8\text{B}$ ,  ${}^{11}\text{C}$ ,  ${}^{14}\text{O}$ ,  ${}^{17,18}\text{F}$ ,  ${}^{20,21}\text{Na}$ ,  ${}^{25}\text{Al}$ ,  ${}^{37}\text{K}$ ,  ${}^{44}\text{Ti}$ ,  ${}^{56}\text{Ni}$ , and others, to improve the understanding of reactions of astrophysical importance. Emphasis focused on “in-flight” production of short-lived ion-species using kinematically inverse reactions on light gaseous targets. Considerable scope still remains for further improving the intensity and quality of these beams in the future, and the beamline is being continually upgraded.
- Make high-precision measurements of nuclear masses with the CPT, particularly the masses of  $N = Z$  nuclei which are of astrophysical interest and are important for testing CVC theory, and measuring the masses of neutron fission fragments that lie close to the anticipated r-process path. Improve the efficiency for production, separation, cooling, transportation, and trap loading of ions to increase sensitivity. Develop the open geometry “Advanced Penning Trap”, the APT.
- Study the shapes, stability and decay modes of nuclei along the proton dripline in order to improve understanding of partially bound nuclei. Study proton tunneling through deformed barriers, in order to increase the spectroscopic information obtained through proton radioactive decay rates. Study the influence of vibrations and coupling to other nucleons in odd-odd systems to generalize the understanding of proton radioactivity. Study excited states in these nuclei using the RDT technique to trigger Gammasphere.
- Study the structure of neutron-rich nuclei in order to understand the modification of shell gaps and the apparent changes in spin-orbit splitting. Study transfer reactions on spherical tin isotopes, the decay and Coulomb excitation of exotic nuclei produced in fragmentation, and the most neutron rich nuclei that can be reached by multi-nucleon transfer and heavy-ion fusion.
- Developing position-sensitive germanium detectors, for “tracking” gamma rays in order to allow the imaging of the source of radiation. The ANL focus is on developing planar germanium wafer technologies, in parallel with involvement in national plans to construct a tracking germanium shell, the GRETINA concept.
- Investigate the collisions and deconfinement of nucleons in nuclear matter at very high temperatures and densities that are achieved in relativistic heavy-ion collisions of gold nuclei at 200 GeV/u. Our participation is using the PHOBOS detector at the RHIC accelerator at Brookhaven National Laboratory.
- Perform detailed R&D studies for the Rare Isotope Accelerator (RIA) and participate in all efforts to refine the designs for the accelerators, target stations, post accelerator, and experimental equipment. Intense effort is being directed to development of the “gas catcher” technology for cooling primary beams.

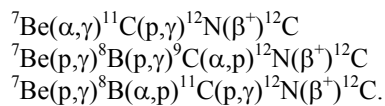
## A. REACTIONS OF ASTROPHYSICAL IMPORTANCE

Research into nuclear reactions that are relevant to astrophysical processes continues to grow and has become a major thrust of our research. A very wide variety of techniques were used this year, exploiting almost all of our equipment, including experiments with radioactive beams, studies with Gammasphere, measurements with the Canadian Penning Trap (CPT), and the use of Accelerator Mass Spectrometry (AMS) for trace element analysis.

### a.1. Studies of the ${}^8\text{B}(\alpha,p){}^{11}\text{C}$ Reaction (K. E. Rehm, C. L. Jiang, J. P. Greene, D. Henderson, R. V. F. Janssens, E. F. Moore, G. Mukherjee, R. C. Pardo, T. Pennington, J. P. Schiffer, S. Sinha, X. D. Tang, R. H. Siemssen, L. Jisonna, R. E. Segel,\* and A. H. Wuosmaa†)

The sequences of nuclear reactions occurring in the early universe, during the Big Bang or in so-called Population III stars, are quite different from the ones observed in present-day stellar nucleosynthesis. The presence of the mass 5 and mass 8 gaps introduces a strong impedance to stellar nucleosynthesis which can only be overcome by  ${}^3\text{He}$  and  $\alpha$  induced reactions.

In most network calculations it is usually assumed that the mass-8 gap is bridged by the triple- $\alpha$  capture reaction which, as a three-body process, requires higher stellar temperatures and densities. It has been argued for some time, however, that other reaction paths could lead to a bypass of the triple- $\alpha$  process, leading to the formation of 'metals' in first generation stars. Making use of hydrogen, deuterium,  ${}^3\text{He}$  and  ${}^4\text{He}$ , produced during the Big Bang, there are three possible sequences leading to the formation of nuclei of mass 12 and beyond. With  ${}^7\text{Be}$  formed via the  ${}^4\text{He}({}^3\text{He},\gamma){}^7\text{Be}$  reaction as a starting point, these three reaction paths are:



Among the six reactions involved in this network, new information about the three (p, $\gamma$ ) reactions was obtained in a variety of recent experiments with radioactive beams or targets. Concerning the three alpha-induced reactions, some information is available for the  ${}^7\text{Be}(\alpha,\gamma){}^{11}\text{C}$  reaction<sup>1</sup> obtained from mirror symmetries and experimental studies of the  ${}^7\text{Be}(\alpha,\gamma){}^{11}\text{C}$  reaction,<sup>2</sup> although the role of sub-threshold resonances in this reaction is not quite clear yet. For the two other

reactions  ${}^8\text{B}(\alpha,\text{p}){}^{11}\text{C}$  and  ${}^9\text{C}(\alpha,\text{p}){}^{12}\text{N}$ , the astrophysical reaction rates are based so far only on Hauser-Feshbach estimates and information from mirror nuclei that are prone to large uncertainties. Because of its lower Coulomb barrier, the  ${}^8\text{B}(\alpha,\text{p}){}^{11}\text{C}$  should have a larger influence in the environment of a population III star. For this reason we performed a first measurement of the astrophysical reaction rate for the  ${}^8\text{B}(\alpha,\text{p}){}^{11}\text{C}$  reaction.

A direct measurement of this reaction requires a  ${}^4\text{He}$  gas target and a low-energy, radioactive ( $T_{1/2} = 0.77\text{s}$ )  ${}^8\text{B}$  beam. Although both are available at ATLAS, the experimental difficulties with this measurement (e.g. low count rates, difficulties with particle identification, etc.) point to a different approach. Because of the large positive Q-value ( $Q = 8.003\text{ MeV}$ ) of the  ${}^8\text{B}(\alpha,\text{p}){}^{11}\text{C}$  reaction, the resonance states in  ${}^{12}\text{N}$  can either be populated with a low energy ( $\sim 4 - 8\text{ MeV}$ )  ${}^8\text{B}$  beam and a  ${}^4\text{He}$  target or through the time-inverse  ${}^{11}\text{C}(\text{p},\alpha){}^8\text{B}$  reaction with a  $\sim 100\text{ MeV}$  radioactive ( $T_{1/2} = 20.4\text{m}$ )  ${}^{11}\text{C}$  beam bombarding a  $\text{CH}_2$  target. Information about the contributions from  ${}^8\text{B}(\alpha,\text{p}){}^{11}\text{C}$  populating excited states in  ${}^{11}\text{C}$  can be obtained through a simultaneous measurement of an excitation function for elastic and inelastic  ${}^{11}\text{C}(\text{p},\text{p}'){}^{11}\text{C}$  scattering.

The experiment was performed with a  ${}^{11}\text{C}$  beam produced via the  $\text{p}({}^{11}\text{B},{}^{11}\text{C})\text{n}$  reaction, using  ${}^{11}\text{B}$  beams of 110 - 120 MeV obtained from the superconducting ATLAS accelerator. An ion-optical system, consisting of a superconducting solenoid mounted directly after the production target, a superconducting resonator to focus the secondary particles in energy, and a  $22^\circ$  bending magnet for separation of the secondary  ${}^{11}\text{C}$  particles from the primary  ${}^{11}\text{B}$  beam, transported the  ${}^{11}\text{C}$

beam to the CH<sub>2</sub> target. About  $2 \times 10^5$  <sup>11</sup>C ions, with energies between 98 - 110 MeV, were incident on the secondary CH<sub>2</sub> foil.

The  $p(^{11}\text{C},p)^{11}\text{C}$  and  $p(^{11}\text{C},\alpha)^8\text{B}$  reactions were measured at nine incident energies covering the excitation energy range of  $E_x = 8.7 - 9.9$  MeV in <sup>12</sup>N. Thick 720- $\mu\text{g}/\text{cm}^2$  polypropylene (CH<sub>2</sub>)<sub>n</sub> foils were used as hydrogen targets. Each measurement thus represents an average over the energy loss in the target (100 keV in the c.m. system) convoluted with the energy spread of the beam. In order to separate scattering of <sup>11</sup>C from scattering of the <sup>11</sup>B beam contaminant, the two outgoing reaction products were detected in kinematic coincidence. The heavy reaction products (<sup>11</sup>B, <sup>11</sup>C and <sup>8</sup>B) were identified with respect to energy  $E$  and nuclear charge  $Z$  in an annular ionization chamber covering the  $\theta_{\text{lab}} = 1.4 - 5^\circ$  angular range. The coincident light particles (protons or alphas) were measured in a Si detector array consisting of two double-sided annular silicon strip detectors covering the angular range  $\theta_{\text{lab}} = 5 - 20^\circ$ . The detectors were segmented in the front and back into 16 rings and 16 wedges, respectively. This array covered, in the c.m. system, the range of  $\theta_{\text{cm}} = 30 - 160^\circ$  with a total detection efficiency of about 70%.

The angular distributions from the  $p(^{11}\text{C},\alpha)^8\text{B}$  reaction measured at the different incident energies were integrated, corrected for detection efficiencies and converted into the  $^8\text{B}(\alpha,p)^{11}\text{C}$  frame. The preliminary

excitation function is given in Fig. I-1, plotted as a function of the excitation energy in the compound nucleus <sup>12</sup>N. The cross sections increase steadily from about 0.05  $\mu\text{b}$  at  $E_x = 8.7$  MeV to 20 mb at  $E_x = 9.9$  MeV. Since the proton threshold in <sup>12</sup>N is at 0.601 MeV, all excited states are particle-unbound. As a result, states at 9 - 10 MeV have generally large proton widths and no resonant structures are observed in the present experiment.

By including the contributions from the population of inelastic channels in the reaction  $p(^{11}\text{C},p)^{11}\text{C}$ , and taking the statistical factors for the inverse reaction into account, the total astrophysical reaction rate for the  $^8\text{B}(\alpha,p)^{11}\text{C}$  reaction can be calculated. The result is shown in Fig. I-2 by the red line in the temperature range  $T_9 = 0.05-0.4$ , where  $T_9$  is the temperature of the stellar environment in  $10^9$  K. The black line is the previous rate, based on a Hauser-Feshbach prediction; it is lower than the experimental result by 1 - 2 orders of magnitude. The reaction rate of the triple-alpha reaction, is smaller than the rate of the  $^8\text{B}(\alpha,p)^{11}\text{C}$  reaction by 12 orders of magnitude. The influence of the hot pp-chain reactions on the formation of <sup>12</sup>C and heavier nuclei through a bypass of the triple- $\alpha$  reactions, however, depends also on many other factors, e.g. on the reaction rate of the  $^7\text{Be}(p,\gamma)^8\text{B}$  reaction, on the <sup>7</sup>Be produced via the  $^3\text{He}(\alpha,\gamma)$  reaction and on the amounts <sup>3</sup>He left over in supermassive stars. For this, complete network calculations in the stellar environments have to be performed. These calculations are presently under way.

\*Northwestern University, †Western Michigan University.

<sup>1</sup>L. Buchmann, J. M. D'Auria, and P. McCorquodale, *Astrophys. J.* **324**, 953 (1988).

<sup>2</sup>G. Hardie *et al.*, *Phys. Rev. C* **29**, 1199 (1984).

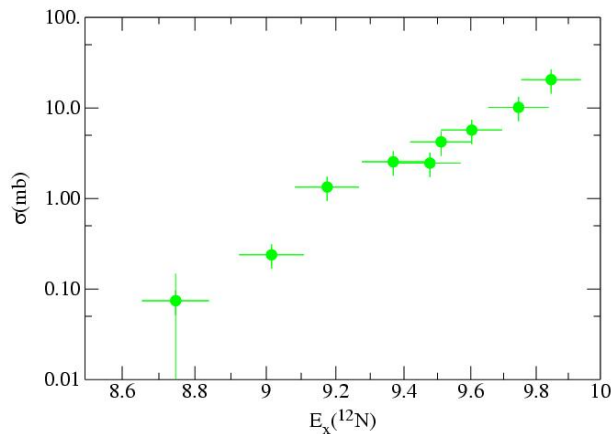


Fig. I-1. Excitation function for the  $^8\text{Be}(\alpha,p)^{11}\text{C}$  reaction plotted as function of the excitation energy in the <sup>12</sup>N compound nucleus.

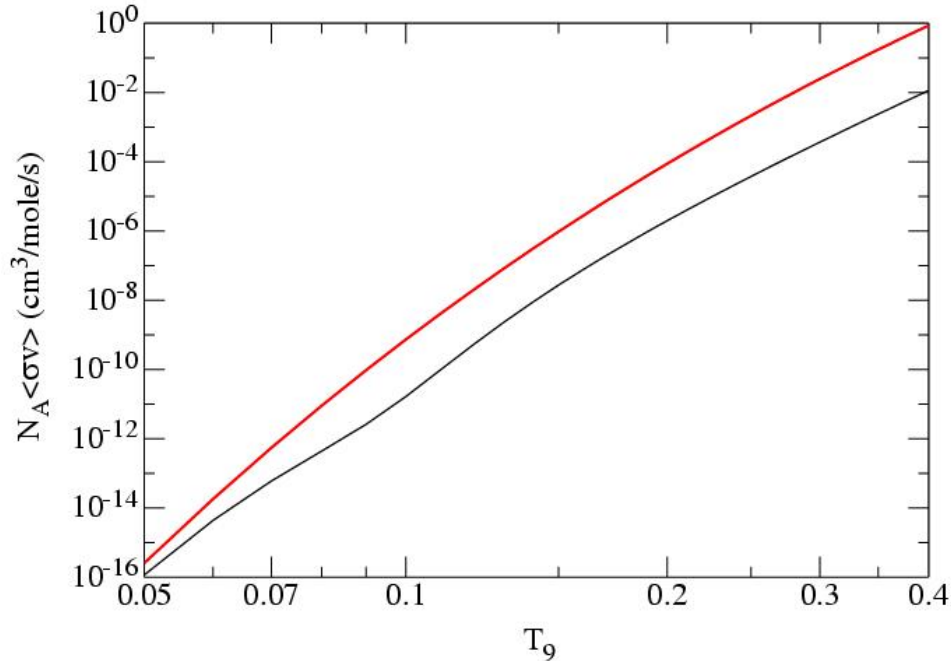


Fig. I-2. Astrophysical reaction rate of the  ${}^8\text{B}(\alpha,p){}^{11}\text{C}$  reaction. Red line: new experimental rate. Black line: rate based on a Hauser Feshbach calculation.

**a.2. Measurement of the  $\beta$ -Delayed  $\alpha$  Spectrum of  ${}^{16}\text{N}$  with a New Technique** (X. Tang, K. E. Rehm, I. Ahmad, J. Greene, A. Hecht, D. Henderson, C. L. Jiang, E. F. Moore, M. Notani, R. C. Pardo, G. Savard, J. P. Schiffer, S. Sinha, M. Paul,\* R. E. Segel,† L. Jisonna,† C. Brune,‡ and A. Wuosmaa§)

The isotopes  ${}^{12}\text{C}$  and  ${}^{16}\text{O}$  are after  ${}^1\text{H}$  and  ${}^4\text{He}$  the third and fourth most abundant nuclei in the visible Universe, and are crucial to all living organisms. Most of the carbon and oxygen is produced by helium burning. The ratio of C/O, which is determined by the competition between the triple- $\alpha$  and  ${}^{12}\text{C}(\alpha,\gamma){}^{16}\text{O}$  reactions, affects not only their own nucleosynthesis but also the future evolution of the star during carbon, neon, and oxygen burning.<sup>1</sup> While the cross section for the triple- $\alpha$  process is experimentally quite well determined<sup>2,3</sup> our knowledge of the  ${}^{12}\text{C}(\alpha,\gamma){}^{16}\text{O}$  reaction under typical helium burning conditions [ $E_{\text{c.m.}} \sim 300$  keV] is still puzzled by a more complicated reaction mechanism.<sup>2,4</sup>

For this reaction, there are two possible  $\alpha$  capture modes. One is E1 capture with contributions from the  $1^-$  state at  $E_r = 2.418$  MeV and the sub-threshold  $1^-$  state at  $E_r = -45$  keV. The other is E2 capture including the contributions from direct capture and a  $2^+(E_r = -245$  keV) sub-threshold state. States with the same angular momentum can interfere with each other.<sup>3</sup> The cross sections at the Gamow window ( $\sim 300$  keV) are so small (of the order of  $10^{-17}$  b) that so far all available direct measurements have been made at energies above  $E_{\text{c.m.}} =$

$0.75$  MeV.<sup>2</sup> These data are then extrapolated into the energy region of interest using R-matrix theory. Since the higher-energy data are not very sensitive to the contributions from sub-threshold resonances, the published S-Factors in the past 30 years range from 1-288 keVb (for S(E1)) and 7-120 keVb (for S(E2)). To improve the reliability of the extrapolations, data from complementary experiments, such as  $\alpha$  scattering off  ${}^{12}\text{C}$ ,  $\alpha$  transfer reactions to  ${}^{12}\text{C}$ , and  ${}^{16}\text{N}$  beta-delayed  $\alpha$  decay were included in the extrapolations.

The beta-delayed  $\alpha$  decay is one of the best methods to determine S(E1). This decay has been studied by two groups.<sup>5,6</sup> Only one of them<sup>6</sup> provides enough experimental details so that the sensitivity to backgrounds and systematic uncertainties can be discussed. In the  $\beta$ -delayed  $\alpha$  decay of  ${}^{16}\text{N}$  the cross section  $\sigma_{\text{E1}}$  is extracted from the height of the shoulder located at  $E = 0.9$  MeV in the  $\alpha$  energy spectrum which is dominated by the decay from the higher-lying  $1^-$  state in  ${}^{16}\text{O}$ . All experiments of  $\beta$ -delayed  $\alpha$ -decay of  ${}^{16}\text{N}$  performed so far have used low-energy  ${}^{16}\text{N}$  beams and Si surface barrier detectors. The high flux of beta

particles in these experiments can lead to distortions of the low-energy part of the alpha spectrum measured with the Si detector. To reduce the sensitivity of the detectors to beta particles, we have built two pairs of gas-filled ionization chambers, for a high-efficiency measurement of the  $\alpha$  and the  $^{12}\text{C}$  recoil which follow the beta delayed decay of  $^{16}\text{N}$  (see Fig. I-3). Compared to Si detectors a gas-filled ionization chamber has a series of advantages:

- (1) it is not subject to a deterioration of the energy resolution which is important especially for longer runs,
- (2) it has smaller pulse height defects and

- (3) it gives generally a better energy resolution.

A 60 MeV  $^{16}\text{N}$  beam has been produced via the  $d(^{15}\text{N},n)^{16}\text{N}$  reaction with a 100pA 70 MeV  $^{15}\text{N}^{5+}$  beam from ATLAS bombarding a  $\text{LN}_2$  cooled deuterium gas target filled with a pressure of 700 mbar. The  $^{16}\text{N}$  ions were separated from the primary beam by a magnetic dipole and focused on the target with a set of two quadrupole magnets. The beam spot on target was restricted to about  $5\text{ mm} \times 5\text{ mm}$  with a 4-jaw collimator mounted in front of the irradiation chamber. The  $^{16}\text{N}$  beam intensity was about 1.2 MHz with a purity of better than 70%. The major beam contaminants were  $^{15}\text{N}$  and  $^{16}\text{O}$ .

\*Hebrew University, Jerusalem, Israel, †Northwestern University, ‡Ohio University, §Western Michigan University.

<sup>1</sup>T. A. Weaver and S. E. Woosley, Phys. Rep. **227**, 65 (1993).

<sup>2</sup>C. E. Rolfs and W. S. Rodney, *Cauldrons in the Cosmos* (University of Chicago, Chicago) 1988.

<sup>3</sup>C. Angulo *et al.*, Nucl. Phys. **A656**, 3 (1999).

<sup>4</sup>L. Buchmann, R. E. Azuma, C. A. Barnes, J. Humblet, and K. Langanke, Phys. Rev. C **54**, 393 (1996).

<sup>5</sup>Z. Zhao *et al.*, Phys. Rev. Lett. **70**, 2066 (1993).

<sup>6</sup>R. E. Azuma *et al.*, Phys. Rev. C **50**, 1194 (1994).

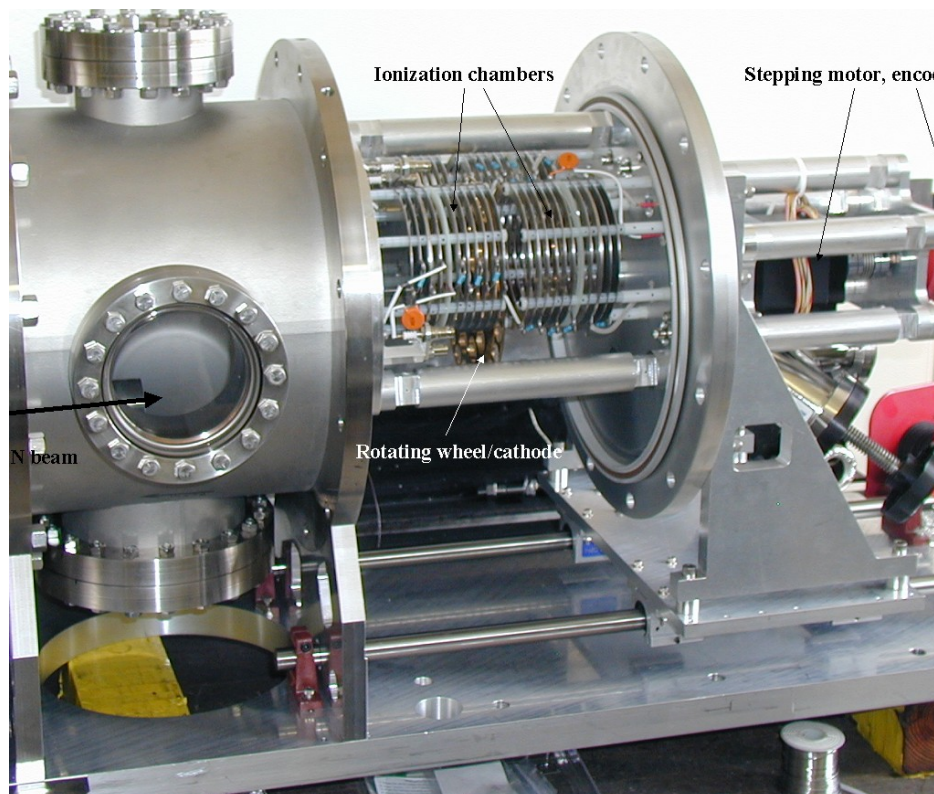


Fig. I-3. Photograph of the experimental setup for measuring the beta-delayed  $\alpha$ -decay of  $^{16}\text{N}$ .

In the irradiation chamber the  $^{16}\text{N}$  ions were slowed down in a 16 cm long gas-filled attenuation cell, with 1.3 mg/cm<sup>2</sup> thick Ti entrance and exit windows. An additional 4.44 mg/cm<sup>2</sup> thick Mylar absorber installed after the attenuation cell reduced the  $^{16}\text{N}$  energy even further. The gas pressure within the attenuation cell was chosen to stop the  $^{16}\text{N}$  particles in the vicinity of a 15  $\mu\text{g}/\text{cm}^2$  thick C catcher foil mounted on a rotating wheel after the attenuation cell. After an irradiation period of 15 s, the wheel was rotated by 120 degree to transport the catcher foil to the center of one pair of ionization chambers for a measurement of the beta-delayed  $\alpha$  decay. During this period a second foil was irradiated which was subsequently measured in the second detector pair. During motion the beam and the data acquisition system was stopped to avoid interference from the electronic noise produced by the stepping motor.

To test the collection efficiency, several thin foils, including carbon, Ti, Al, TiN, and melamine with thicknesses ranging from 10  $\mu\text{g}/\text{cm}^2$  to 50  $\mu\text{g}/\text{cm}^2$ , were mounted on the wheel. A Si detector was installed at 180 degree relative to the irradiation position to detect the betas from the  $^{16}\text{N}$  decay. By varying the pressure of the gas attenuation cell, the beta activity was measured as function of the gas pressure. To normalize the data, a thick Al target was used to stop all  $^{16}\text{N}$  ions transmitted through the gas and this beta activity was

used for normalization. The collection efficiency was found to be independent of the chemical properties of the foil. For a 15  $\mu\text{g}/\text{cm}^2$  C foil, the efficiency is about 5-6%. A 50  $\mu\text{g}/\text{cm}^2$  C foil has an efficiency as large as 20%. However, the large energy loss of the recoiling  $^{12}\text{C}$  ions prevented the use of this foil.

The long-term stability of the system was tested in various  $\alpha$  and  $^{16}\text{N}$  test experiments. A preliminary summed alpha spectrum from the four ionization chambers obtained in a 17 hour long run with  $^{16}\text{N}$  is shown in Fig. I-4. A cut on the pulse height ratio between alpha and  $^{12}\text{C}$  recoil has been applied to every ionization chamber. The alpha energy was calibrated with 3.18 MeV alphas from a  $^{148}\text{Gd}$  source. The asymmetrical shape of the major peak arises from the alpha energy loss in the catcher foil and has been well reproduced with a detailed Monte Carlo calculation. The events around 0.9 MeV originate from the interference with the subthreshold  $1^-$  state. The remaining background in this region is caused by the asymmetric wheel structure which results in stopping some of the alpha particles in the material around the catcher foils. A planned modification of the wheel will minimize this background. The alpha- $^{12}\text{C}$  coincidence rate from the two pairs of ionization chambers obtained so far was about 11/min. With planned improvements of the transport efficiency we expect to collect about  $5 \times 10^5$  coincidence events in a week-long run.

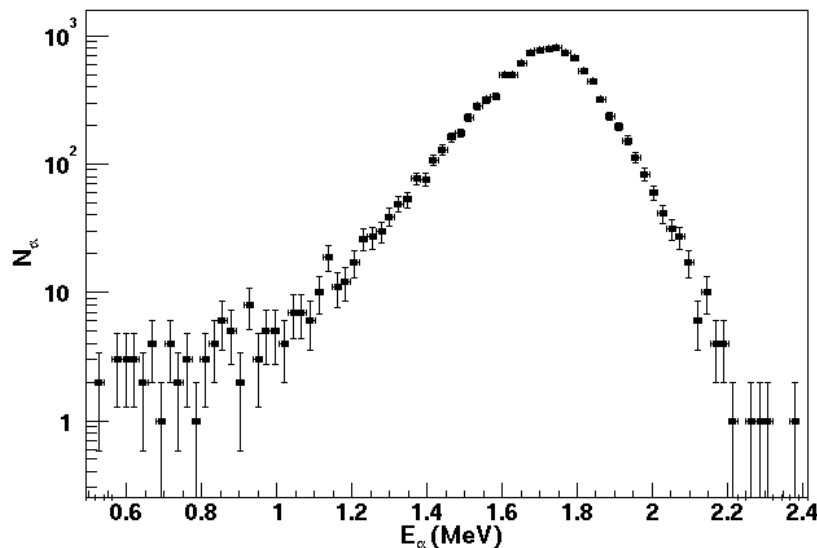
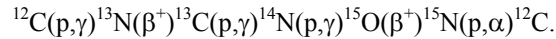


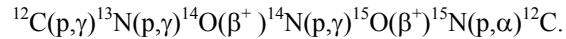
Fig. I-4. A preliminary summed alpha spectrum from the  $^{16}\text{N}$  decay detected by the four ionization chambers. A cut on the pulse height ratio between alpha and  $^{12}\text{C}$  recoil has been applied to the ionization chamber signals to generate this spectrum.

**a.3 Study of the Breakout Reaction  $^{18}\text{Ne}(\alpha, p)^{21}\text{Na}$**  (S. Sinha, J. Greene, D. Henderson, R. V. F. Janssens, C. L. Jiang, E. F. Moore, R. C. Pardo, K. E. Rehm, J. P. Schiffer, X. Tang, A. Chen,\* L. Jissonna,† R. Segel,‡ R. H. Siemssen,‡ and A. H. Wuosmaa§)

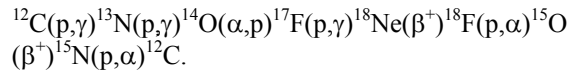
Radioactive ion beam facilities provide low-energy beams to measure the cross sections of astrophysically important reactions. One of the current challenges is determining the reaction rates of various breakout processes from the hot CNO (HCNO) cycles leading to the rapid proton capture process (rp process). The HCNO cycles and rp process are the main energy source in explosive hydrogen burnings and a source for the nucleosynthesis of heavier elements. Explosive hydrogen and helium burning takes place most notably in cataclysmic binary systems, such as in novae, x-ray busters, and type I supernovae.<sup>1</sup> In the normal CNO cycle, the principal reaction sequence converts four hydrogen nuclei into an alpha particle.<sup>2,3</sup>



At temperatures,  $T \sim 0.2$  GK, the  $^{13}\text{N}(p,\gamma)^{14}\text{O}$  reaction becomes more dominant bypassing the  $^{13}\text{N}(\beta^+)^{13}\text{C}$  decay. This gives rise to the so-called Hot CNO cycle



At temperatures  $T \sim 0.4$  GK, the slow  $^{14}\text{O}(\beta + \nu)^{14}\text{N}$  decay is again bypassed, giving rise to the series:



The breakout from the HCNO cycle and the onset of the rp process at higher temperatures is dependent on the

reaction rates of reaction paths such as  $^{18}\text{F}(p,\gamma)^{19}\text{Ne}$ ,  $^{15}\text{O}(\alpha,\gamma)^{19}\text{Ne}$  and  $^{18}\text{Ne}(\alpha,p)^{21}\text{Na}$ .

In the recent past, new information regarding the astrophysical rates of these reactions were reported.<sup>4-6</sup> While at lower temperatures the first two reactions are the dominant breakout routes, at temperatures in the region of  $T_9 \sim 1$  to 2 Gk and densities of  $\rho \sim 10^3 - 10^6$  g/cm<sup>3</sup> the breakout from CNO cycle starts to be influenced by the  $^{18}\text{Ne}(\alpha,p)^{21}\text{Na}$  reaction. A direct measurement of the  $^{18}\text{Ne}(\alpha,p)^{21}\text{Na}$  reaction is difficult, since it requires a radioactive  $^{18}\text{Ne}$  beam and a  $^4\text{He}$  gas target. During the last two years, two direct measurements of the  $^{18}\text{Ne}(\alpha,p)^{21}\text{Na}$  were reported.<sup>7,8</sup> In both measurements, a post-accelerated  $^{18}\text{Ne}$  beam was produced at the radioactive ion beam facility at Louvain-Na-Neuve bombarding a helium-filled target cell. The excitation energy region covered the range from  $E_x = 1.7 - 3.01$  MeV, which is too high to significantly influence stellar nucleosynthesis.

From the resonance strengths  $\omega\gamma = \omega\Gamma_\alpha[\Gamma_p/\Gamma_{\text{total}}]^{7,8}$  one can extract lower limits for the alpha widths  $\Gamma_\alpha$ . Comparing these widths with the corresponding Wigner limits one observes that most of the high lying states observed<sup>8</sup> have spectroscopic factors around 1, while typically values of 0.01 are expected at these excitation energies. In order to study this discrepancy in more detail we performed two experiments with  $^{21}\text{Na}$  beams at ATLAS.

\*McMaster University, Ontario, Canada, †Northwestern University, ‡Kernfysisch Versneller Instituut, Groningen, Netherlands, §Western Michigan University.

<sup>1</sup>A. E. Champagne *et al.*, *Annu. Rev. Nucl. Part. Sci.* **42**, 39 (1992).

<sup>2</sup>M. Wiescher *et al.*, *J. Phys. G: Nucl. Part. Phys.* **25**, 133(1999).

<sup>3</sup>R. K. Wallace *et al.*, *Astrophys. J. Suppl.* **45**, 389(1981).

<sup>4</sup>K. E. Rehm *et al.*, *Phys. Rev. C* **55**, R566 (1997).

<sup>5</sup>B. Davids *et al.*, *Phys. Rev. C* **67**, 012801 (2003).

<sup>6</sup>K. E. Rehm *et al.*, *Phys. Rev. C* **67**, 065809 (2003).

<sup>7</sup>W. Bradfield-Smith *et al.*, *Phys. Rev. C* **59**, 3402 (1999).

<sup>8</sup>D. Groombridge *et al.*, *Phys. Rev. C* **66**, 055802 (2002).



Through detailed balance the time-inverse  $^{21}\text{Na}(p,\alpha)^{18}\text{Ne}$  reaction is related to the  $^{18}\text{Ne}(\alpha,p)^{21}\text{Na}$  reaction studied previously at Louvain-la-Neuve as long as the resonant state in the compound nucleus  $^{22}\text{Mg}$  decays to the ground state of  $^{21}\text{Na}$ . Among the states<sup>8</sup> the  $2^+$  state at  $E_x = 2.51 \pm 0.14$  MeV was found to decay predominantly to the ground state in  $^{21}\text{Na}$  with a peak cross section of  $\sigma_{\text{lab}} = 42$  mb. We therefore studied the  $^{21}\text{Na}(p,\alpha)^{18}\text{Ne}$  reaction at an energy slightly above this resonance. In a second experiment we also tried to extend the measurement of the  $^{21}\text{Na}(p,\alpha)^{18}\text{Ne}$  excitation function towards lower excitation energies ( $E_x = 1.6 - 2.1$  MeV).

The experiment was performed at the ATLAS accelerator with a  $^{21}\text{Na}$  beam produced by the in-flight technique. A primary beam of  $^{20}\text{Ne}$  with energies of 135 - 145 MeV bombarded a liquid-nitrogen-cooled, 3.5 cm long gas target, filled with  $\approx 0.8$  atm of  $\text{D}_2$  gas. A small fraction of the beam was converted into  $^{21}\text{Na}$  ions via the  $d(^{20}\text{Ne},^{21}\text{Na})n$  reaction and emitted from the gas cell in a cone with opening angle of  $4^\circ$  with respect to the beam direction. A superconducting solenoid refocused the  $^{21}\text{Na}$  particles, and superconducting resonators before and after the gas cell reduced the energy spread of the beam. The  $^{21}\text{Na}^{+11}$  ions were separated from the primary  $^{20}\text{Ne}$  beam with a bending magnet and refocused onto a  $5 \times 5$  mm<sup>2</sup> beam spot. About  $\approx 5000$  particles/sec of  $^{21}\text{Na}$  were incident on the target. The energy resolution was limited by the energy loss of the  $^{21}\text{Na}$  ions in the  $360$   $\mu\text{g}/\text{cm}^2$  thick  $\text{CH}_2$  target

to about 140 keV in the center-of-mass of the  $^{18}\text{Ne} + \alpha$  system.

The experimental setup consisted of two position-sensitive, double-sided, annular silicon strip detectors mounted at forward angles to measure the energy ( $E_\alpha$ ) and angle ( $\theta_\alpha$ ) of the scattered light particles (p or  $\alpha$ ). The heavier particles ( $^{20}\text{Ne}$ ,  $^{21}\text{Na}$  and  $^{18}\text{Ne}$ ) were detected in an annular gas detector system consisting of a Parallel Plate Avalanche Counter and a Bragg ionization chamber. The energy and the beam purity of the secondary beam were monitored throughout the experiment with the focal plane detector of the Enge Spectrograph which was also used for beam normalization purposes. Another beam normalization was done with a Ge detector which counted the 511- $\gamma$  rays emitted from the  $\beta^+$ -decay of  $^{21}\text{Na}^{11+}$ .

In the analysis a kinematic coincidence was required between an  $\alpha$ -particle, detected in the double-sided annular strip detectors, covering the angular range  $\sim 5^\circ - 20^\circ$  and a  $^{18}\text{Ne}$  ion identified with respect to energy and nuclear charge  $Z$  in the Bragg Ionization chamber covering the angular coverage from  $1^\circ - 6^\circ$ . Figure I-5 shows a plot of scattering angle  $\theta_\alpha$  vs.  $\alpha$  energy  $E$  for  $\alpha - ^{18}\text{Ne}$  coincidence events. The solid line indicates the expected kinematic behavior for the reaction  $^{21}\text{Na}(p,\alpha)^{18}\text{Ne}$  at an energy  $E_{\text{lab}} = 113.2$  MeV. The majority of the events are clearly consistent with the reaction of interest.

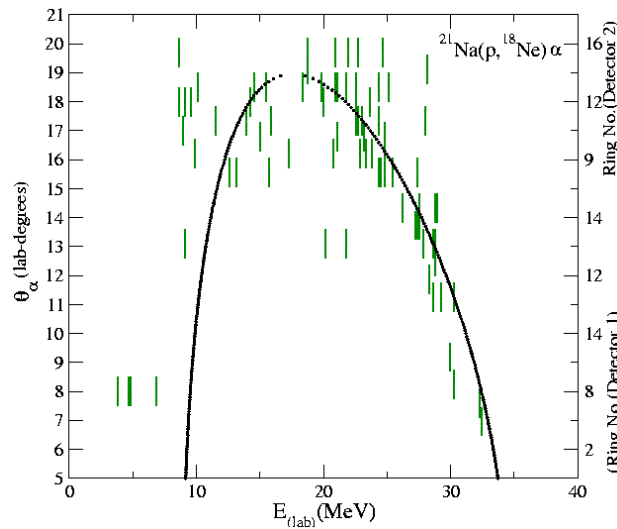


Fig. I-5. Scatter plots of scattering angle  $\theta_\alpha(\text{lab})$  (ring number) vs. energy of  $\alpha$  particles for  $\alpha - ^{18}\text{Ne}$  coincidence events. The solid line indicates the expected kinematic behavior for the reaction  $^{21}\text{Na}(p,\alpha)^{18}\text{Ne}$  at an energy  $E_{\text{LAB}} = 113.2$  MeV.

Assuming an isotropic angular distribution the data were converted into angle-integrated cross sections and transformed into the  $^{18}\text{Ne}(\alpha,p)^{21}\text{Na}$  reference system. They are presented as a function of the center-of-mass energy  $E_\alpha$  in Fig. I-6. The uncertainties of these preliminary cross sections are purely statistical. As can be seen from Fig. I-6 the cross sections obtained from the  $^{21}\text{Na}(p,\alpha)^{18}\text{Ne}$  reaction at  $E_x = 2.51$  MeV is smaller

than the direct measurement<sup>8</sup> by a factor of about 50 resulting in an alpha width which is only a few percent of the Wigner limit. For the measurement at lower energies so far only upper limits for the cross sections can be given, which, at the highest energies, are again smaller than the results.<sup>7</sup> Monte Carlo simulations are presently being performed to study the effects of systematic uncertainties.

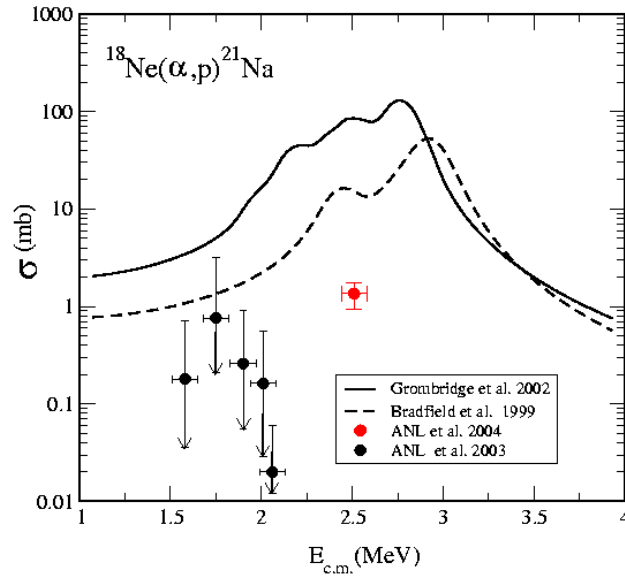


Fig. I-6. Angle-integrated cross sections for  $^{21}\text{Na}(p,\alpha)^{18}\text{Ne}$  transformed into the  $^{18}\text{Ne}(\alpha,p)^{21}\text{Na}$  reference system using the principle of detailed balance shown by filled circles. The solid and dashed lines are the direct measurements of Louvain-La-Neuve (Ref. 7, Ref. 8).

**a.4. Complete Spectroscopy of  $^{20}\text{Na}$  Below the Proton Threshold** (D. Seweryniak, M. P. Carpenter, N. Hammond, A. Heinz, R. V. F. Janssens, T. L. Khoo, C. J. Lister, G. Mukherjee, E. Rehm, S. Sinha, S. J. Freeman,\* J. Shergur,† P. J. Woods,‡ B. Blank,§ T. Davinson,‡ J. Goerres,|| N. Hoteling,¶ D. G. Jenkins,\*\* H. Mahmud,‡ Z. Liu,‡ F. Sarazin,‡ M. Shawcross,|| and A. Woehr¶)

The  $^{20}\text{Na}$  nucleus is part of the sequence  $^{15}\text{O}(\alpha,\gamma)^{19}\text{Ne}(p,\gamma)^{20}\text{Na}$  which is thought to dominate the breakout from the hot CNO cycles into the rp-process in X-ray bursters.

The  $^{10}\text{B}(^{12}\text{C},2n)$  reaction was used to populate excited states in  $^{20}\text{Na}$ . Prompt  $\gamma$  rays were detected using the Gammasphere array of Compton suppressed Ge detectors. The residues were mass dispersed in the Argonne Fragment Mass Analyzer and selected

according to their atomic numbers based on the  $E-\Delta E$  measurement in an ionization chamber. This experiment was a continuation of the earlier studies performed with only 2 clover detectors and an array of BGO scintillators. The level scheme proposed for  $^{20}\text{Na}$  is shown in Fig. I-7, together with the partial level scheme of the mirror nucleus  $^{20}\text{F}$ . Detailed results were published.<sup>1</sup>

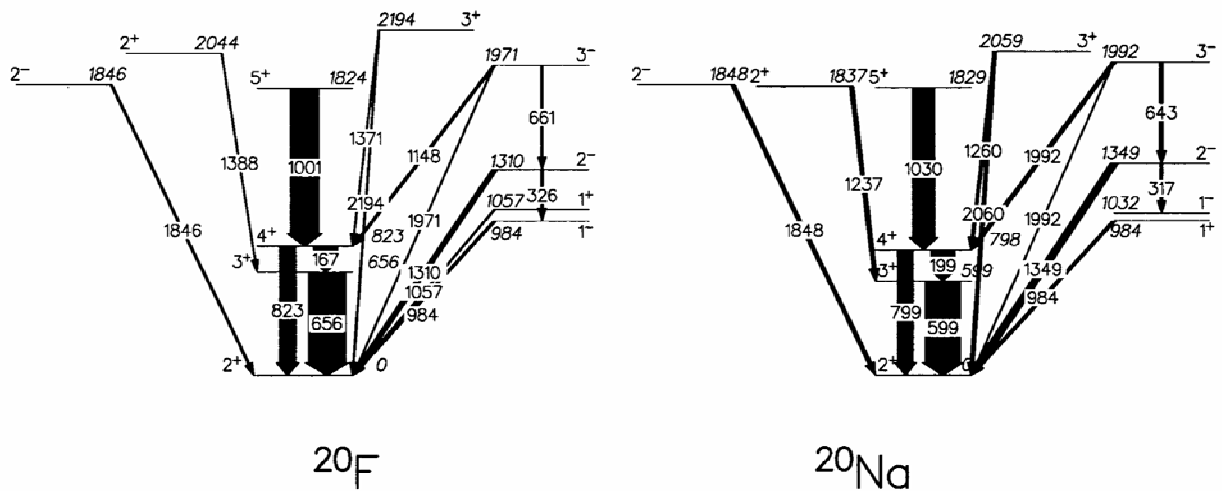


Fig. I-7. Proposed  $^{20}\text{Na}$  and partial  $^{20}\text{F}$  level schemes.

All subthreshold states were observed in  $^{20}\text{Na}$  as compared with its mirror  $^{20}\text{F}$  produced in the same experiment. The lowest known state above the particle threshold in  $^{20}\text{Na}$  is at an excitation energy of 2645(6) keV. It is the most important resonance for determining the  $^{19}\text{Ne}(p,\gamma)^{20}\text{Na}$  reaction rate in X-ray burster scenarios. The nature of this state has been a matter of debate for over a decade. Assuming a  $3^+$  assignment for the 2645(6) keV state, a  $\gamma$  branch with a transition energy around 1847(6) keV would be expected to the  $4^+$  state at 799 keV. Indeed, a transition with 42 counts is found at 1848 keV, but it is not found to be in coincidence with other  $\gamma$  transitions ruling this interpretation out as the dominant origin for this activity. As a result, this transition was interpreted as connecting the  $2^-$  state with the ground state rather than deexciting the 2643-keV state. The alternative  $1^+$  assignment of the 2645-keV level would imply a 90% proton decay branch, with a single strong  $\gamma$ -decay branch (based on the decay of the analogue state in  $^{20}\text{F}$ ) to the  $1^-$  state in  $^{20}\text{Na}$  with a transition energy of around 1613(6) keV. No such transition is observed.

The present data on sub-threshold states are in excellent agreement with the suggested assignments of Ref. 2. A

particular feature is the relative stability of the negative parity states in the mirror system. Shell Model calculations, and semi-empirical calculations based on the Isobaric Mass Multiplet Equation (IMME), were previously presented by Lamm *et al.*<sup>3</sup> concerning the excitation energies of states in  $^{20}\text{Na}$ . Comparing these calculations with the present new data, we confirm that the (sd) space shell model calculation is able to give reasonable agreement with the sub-threshold positive parity states. However, all the sub-threshold negative parity states are much higher in energy than the shell model calculations performed within the (psd) space predicted.<sup>3</sup>

It is important both for the present case of  $^{20}\text{Na}$ , and other neighboring astrophysically important nuclei near the proton drip-line, that a consistent theoretical understanding of level structures in this region is obtained. In that respect the present high quality, comprehensive data provide a useful constraint on future calculations.

\*Argonne National Laboratory and University of Manchester, United Kingdom, †Argonne National Laboratory and University of Maryland, ‡University of Edinburgh, United Kingdom §CEN Bordeaux-Gradignan, IN2P3-CNRS, France, ¶University of Maryland, ||University of Notre Dame, \*\*University of York, Heslington, United Kingdom.

<sup>1</sup>D. Seweryniak, P.J. Woods *et al.*, Phys. Lett. **B590**, 170 (2004).

<sup>2</sup>B. A. Brown *et al.*, Phys. Rev. C **48**, 1456 (1993).

<sup>3</sup>L. O. Lamm *et al.*, Nucl. Phys. **A510**, 503 (1990).

**a.5. Reevaluation of the  $^{22}\text{Na}(p,\gamma)$  Reaction Rate: Implications for the Detection of  $^{22}\text{Na}$  Gamma Rays from Novae** (D. G. Jenkins, C. J. Lister, R. V. F. Janssens, T. L. Khoo, E. F. Moore, K. E. Rehm, B. Truett, A. H. Wuosmaa, M. Freer,\* B. R. Fulton,† and J. Jose‡)

Understanding the formation and destruction of nuclei in the cosmos is a central topic for contemporary nuclear astrophysics. Measuring critical reaction rates is a key element vital to making progress in this field.  $^{22}\text{Na}$  is a short-lived product from novae which has a decay gamma ray that might be observable from the new generation of space-based gamma-ray observatories. Consequently, the formation and destruction of this element is of current significance. The destruction through the  $^{22}\text{Na}(p,g)$  reaction is not

well known, as  $^{22}\text{Na}$  is not stable. We formed the critical states in the Gamow window of  $^{23}\text{Mg}$  using the  $^{12}\text{C}(^{12}\text{C},n)^{23}\text{Mg}$  reaction. Excitation energies, lifetimes, spins and parities were extracted, allowing the reaction rate to be re-evaluated. The new rate shows  $^{22}\text{Na}$  is destroyed faster than was previously expected, so has a lower abundance after a nova explosion, and will be consequently harder to detect than was previously thought. This research was published as a Physical Review Letter.<sup>1</sup>

\*University of Birmingham, United Kingdom, †University of York, United Kingdom, ‡University of Barcelona, Spain

<sup>1</sup>D. G. Jenkins *et al.*, Phys. Rev. Lett. **92**, 031101 (2004).

**a.6. The Level Structure and Mass of  $^{22}\text{Mg}$**  (D. Seweryniak, M. P. Carpenter, N. Hammond, A. Heinz, R. V. F. Janssens, T. L. Khoo, C. J. Lister, G. Mukherjee, E. Rehm, S. Sinha, P. J. Woods,\* B. Blank,† T. Davinson,\* S. J. Freeman,‡ J. Goerres,§ N. Hoteling,¶ D. G. Jenkins,|| H. Mahmud,\* Z. Liu,\* F. Sarazin,\* J. Shergur,\*\* M. Shawcross,§ and A. Woehr¶)

The light  $T_z = -1$  nuclei adjacent to the proton dripline play an important role in explosive stellar environments. Properties of the states situated just above the proton threshold, which can be resonantly populated in  $(p,\gamma)$  reactions, are of special interest. The properties of  $^{22}\text{Mg}$  determine the production of the interstellar  $\gamma$  emitter  $^{22}\text{Na}$  as part of the NeNa cycle.

The single largest contributor to the  $^{21}\text{Na}(p,\gamma)^{22}\text{Mg}$  reaction rate under novae burning conditions is thought to be from resonant capture on a  $2^+_{4}$  excited state. The level at 5714.4(15) keV was first identified in 1972 by Rolfs *et al.*<sup>1</sup> by its  $\gamma$  decay, and subsequently confirmed by Grawe *et al.*, with an energy 5713(2) keV<sup>2</sup> giving a weighted value of 5713.9(12) keV. The associated resonance strength was recently measured with the DRAGON spectrometer at the ISAC facility.<sup>3</sup> However, a significant discrepancy emerged between

the precisely measured resonance energy of 205.7(5) keV and the value of 212 keV anticipated from the tabulated values of the  $^{22}\text{Mg}$  and  $^{21}\text{Na}$  masses.<sup>3</sup> It was suggested by Hardy *et al.* that this may be due to the need for a re-evaluation of the  $^{22}\text{Mg}$  mass.<sup>4</sup>

The  $^{12}\text{C}(^{12}\text{C},2n)$  reaction was used to learn more about the resonant states and the structure of the  $^{22}\text{Mg}$  nucleus. Prompt  $\gamma$  rays were detected using the Gammasphere array of Compton suppressed Ge detectors. The residues were mass dispersed in the Argonne Fragment Mass Analyzer and selected according to their atomic numbers based on the  $E-\Delta E$  measurement in an ionization chamber. The  $\gamma$ -ray spectrum measured in coincidence with the  $^{22}\text{Mg}$  residues is shown in Fig. I-8. Figure I-9 shows the proposed  $^{22}\text{Mg}$  level scheme.

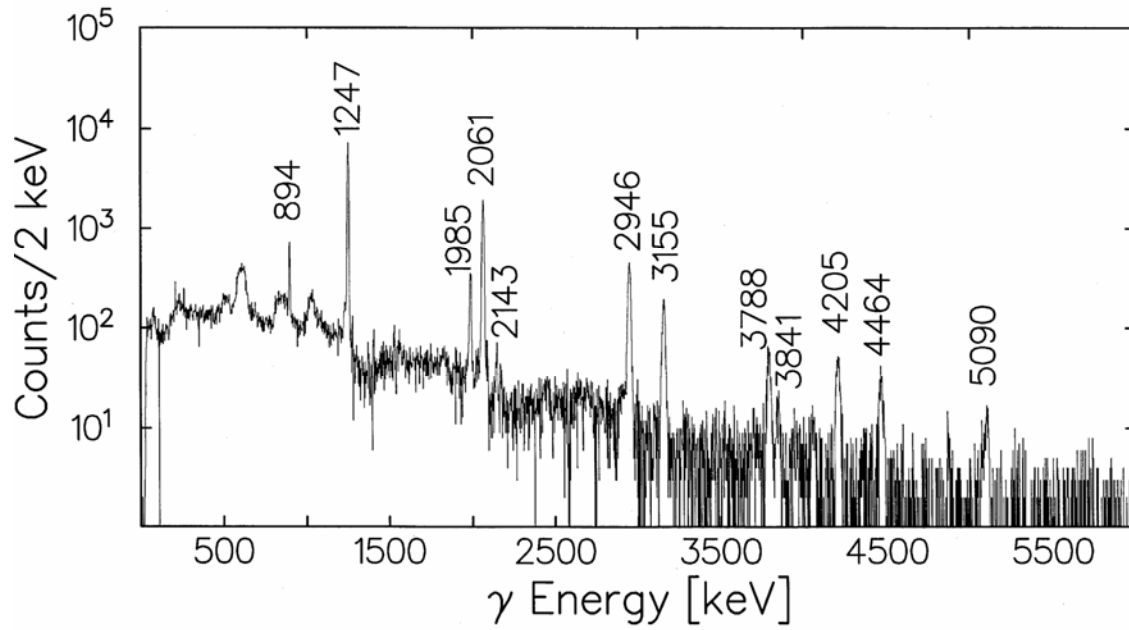


Fig. I-8. Gamma-ray spectrum detected in coincidence with  $^{22}\text{Mg}$  nuclei.

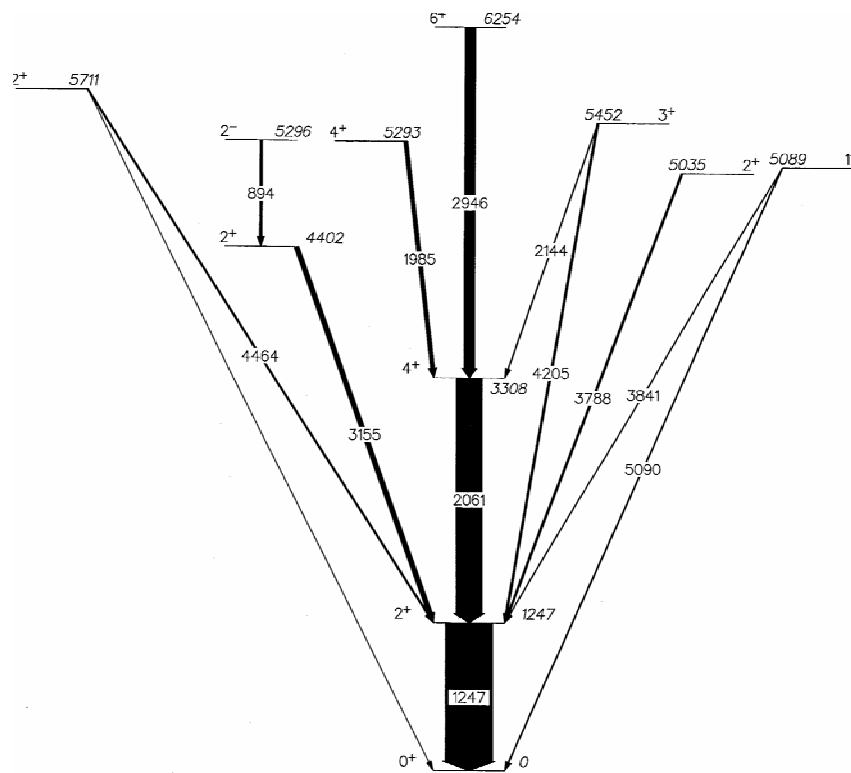


Fig. I-9. The proposed  $^{22}\text{Mg}$  level scheme.

The important  $2^+_4$  resonance<sup>1</sup> was observed and its  $\gamma$ -decay properties were measured. Based on the comparison with the mirror nucleus  $^{22}\text{Ne}$  all states below the proton threshold were observed. In addition, a new  $6^+$  state at 6254 keV above the proton threshold was proposed.

The  $3^-$  level is the only mirror level yet to be identified in this energy region. Assuming the same mirror energy shift for the  $3^-$  state as for the only other  $2^-$  negative parity state identified in the present study, gives an energy of 6059 keV, very close to a level at 6046 keV, previously assigned as  $1^-$ .<sup>5</sup> Taking the recent  $(p,\gamma)$  resonance strength measurement of<sup>6</sup> gives a partial half-life of about 35 fs in excellent agreement with the mirror transition value of 32(9) fs, supporting the  $3^-$  assignment for the 6046 keV level.

The measured energy of the  $2^+_4 \rightarrow 2^+_1$  transition leads to an excitation energy of 5711.0(10) keV, which disagrees with the tabulated value. Taking the resonance energy measured in Ref. 3, and using the  $^{21}\text{Na}$  mass value from Audi *et al.*,<sup>7</sup> combined with the

new excitation energy value gives a  $^{22}\text{Mg}$  mass excess of -400.5(13) keV, in agreement with the revised value of -402(3) keV suggested in Ref. 4, and with recent high precision values of -399.92(27) keV<sup>8</sup> and -399.64(63) keV<sup>9</sup> measured at CERN and Argonne, respectively. The present measurement of the  $^{22}\text{Mg}$  mass leads to a derived Ft value for the superallowed Fermi transition of 3082.3(9.5)s<sup>10</sup> (the mass of  $^{22}\text{Na}$  from Ref. 7 was used in the calculations), which compares well with the expected CVC hypothesis value of 3072.3(8) s.

In conclusion, modern in-beam  $\gamma$  spectroscopic techniques enabled us to make a full structure determination of  $^{22}\text{Mg}$ , both below the proton threshold and in the region relevant for astrophysical burning. We conclude that no further measurements of the  $^{21}\text{Na}(p,\gamma)^{22}\text{Mg}$  reaction are needed to determine resonant reaction rates under novae conditions. The new precise measurement of the  $\gamma$ -ray energy from the most important astrophysical resonance is used to derive a  $^{22}\text{Mg}$  mass value.

\*University of Edinburgh, United Kingdom, †CEN Bordeaux-Gradignan, France, ‡Argonne National Laboratory and University of Manchester, United Kingdom, §University of Notre Dame, ¶University of Maryland, ||University of York, Heslington, United Kingdom, \*\*Argonne National Laboratory and University of Maryland.

<sup>1</sup>C. Rolfs *et al.*, Nucl. Phys. **A191**, 209 (1972).

<sup>2</sup>H. Grawe *et al.*, Nucl. Phys. **A237**, 18 (1975).

<sup>3</sup>S. Bishop *et al.*, Phys. Lett. **90**, 162501 (2003).

<sup>4</sup>J. C. Hardy *et al.*, Phys. Rev. Lett. **91**, 082501 (2003).

<sup>5</sup>B. Davids *et al.*, Phys. Rev. C **68**, 055805 (2003).

<sup>6</sup>J. D'Auria *et al.*, Phys. Rev. C **69**, 065803 (2004).

<sup>7</sup>A. H. Wapstra, G. Audi, and C. Thibault, Nucl. Phys. **A729**, 129 (2003).

<sup>8</sup>M. Mukherjee *et al.*, Phys. Rev. Lett., in print.

<sup>9</sup>G. Savard *et al.*, submitted to Phys. Rev. C.

<sup>10</sup>I. S. Towner and J. C. Hardy, private communication (2004).

### a.7. Measurement of $^{44}\text{Ti}$ Half-Life (I. Ahmad, J. P. Greene, E. F. Moore, W. Kutschera,\* and M. Paul†)

The half-life measurement of  $^{44}\text{Ti}$ , which was started in March 1992, is being continued at Argonne and Jerusalem with the aim of reducing systematic uncertainties. The half-life determined from 5 years decay was published<sup>1</sup> in 1998. The half-life is being

determined by measuring spectra of a mixed source of  $^{44}\text{Ti}$  and  $^{60}\text{Co}$  with a 25% Ge detector at regular intervals. The data, which covers 11 years, are being analyzed and the results will be published by the end of the year.

\*University of Vienna, Austria, †Hebrew University, Jerusalem, Israel.

<sup>1</sup>I. Ahmad *et al.*, Phys. Rev. Lett. **80**, 2550 (1998).

- a.8. Stellar  $^{62}\text{Ni}(n,\gamma)^{63}\text{Ni}$  Reaction** (I. Ahmad, J. P. Greene, D. J. Henderson, C. L. Jiang, R. C. Pardo, T. Pennington, K. E. Rehm, R. Scott, S. Sinha, X. Tang, R. Vondrasek, H. Nassar,\* M. Paul,\* S. Ghelberg,\* S. Dababneh,† M. Heil,† F. Käppeler,† R. Plag,† R. Reifarh,‡ A. Heger,‡ H. Koivisto,§ P. Collon,¶ S. O'Brien,¶ M. Bettan,|| D. Berkovits,|| and N. Patronis\*\*)

The overestimate of neutron-rich Ni isotope production by a factor of  $\sim 10$  (compared to solar abundances) in stellar-nucleosynthesis calculations may be connected to uncertainties in  $(n,\gamma)$  cross sections. The  $^{62}\text{Ni}(n,\gamma)^{63}\text{Ni}$  ( $t_{1/2} = 100 \pm 2$  yrs) reaction is considered important. The cross section  $\sigma_V$  of this reaction at stellar temperatures was measured by activating an enriched  $^{62}\text{Ni}$  target with an integrated neutron flux  $\phi_V t$  having a quasi-Maxwellian ( $kT = 25$  keV) velocity distribution and measuring the  $^{63}\text{Ni}/^{62}\text{Ni}$  isotopic ratio  $r = \sigma_V \phi_V t$  by accelerator mass spectrometry (AMS). The

activation was performed at Karlsruhe, using neutrons from the  $^7\text{Li}(p,n)^7\text{Be}$  reaction just above threshold. The AMS measurements were performed at the ATLAS facility (Argonne). Ni was fed into the electron-cyclotron-resonance (ECR) ion source in gas phase as organo-metallic nickelocene synthesized at Jyväskylä from the activated Ni metal.  $^{63}\text{Ni}^{15+}$  ions were accelerated to 9.2 MeV/n and the gas-filled magnet technique was used to separate the extremely intense isobaric  $^{63}\text{Cu}$  background contaminant (Fig. I-10). The count rate of identified  $^{63}\text{Ni}$  ions, corrected for

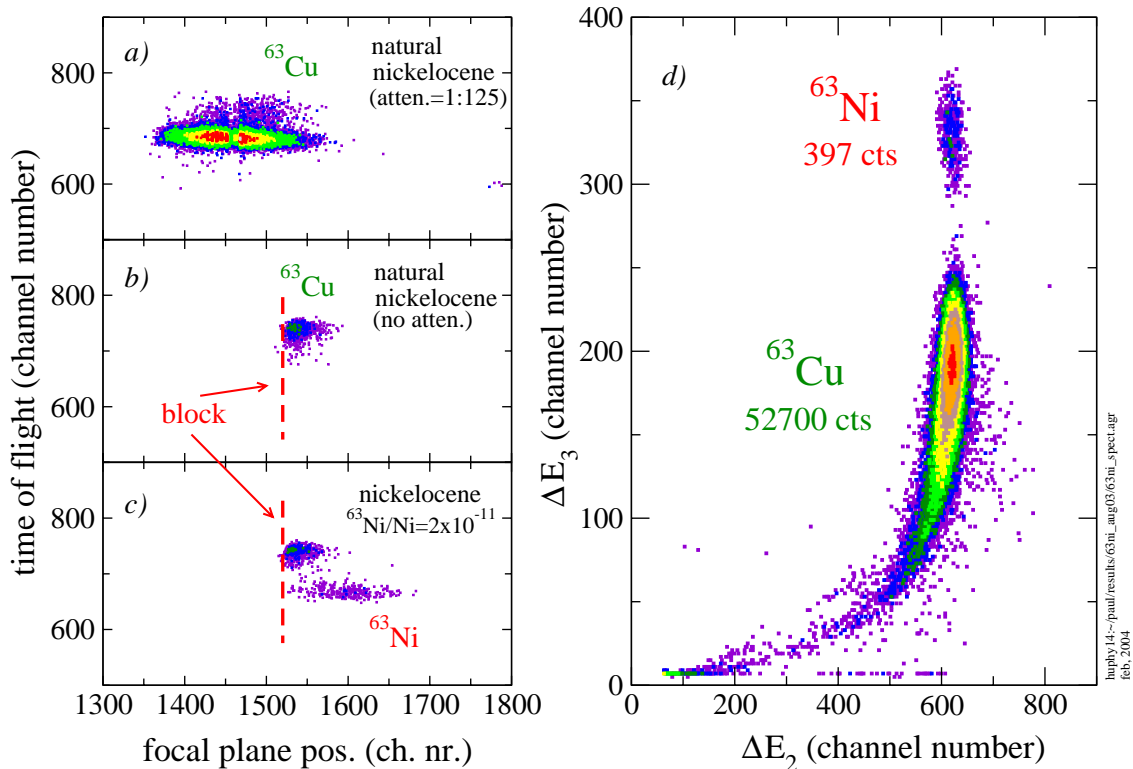


Fig. I-10. (left) Time-of-flight versus focal plane position two-dimensional spectra showing the separation between  $^{63}\text{Ni}$  and the isobaric contaminant  $^{63}\text{Cu}$ ; (right) identification spectrum ( $\Delta E_3$  versus  $\Delta E_2$ ) measured in the focal-plane multi-anode ionization chamber.

ion transmission and divided by the Ni ion intensity at the ECR source, determines the  $^{63}\text{Ni}/^{62}\text{Ni}$  ratio (down to the  $10^{-13}$  range) in the Ni source feed. To reduce systematic uncertainties, the ratio was normalized to that measured in the same conditions for a thermal-neutron activation of  $^{62}\text{Ni}$ , using the known thermal-neutron capture cross section  $\sigma_{\text{th}}(^{62}\text{Ni}) = 14.2 \pm 0.3$  b

(Fig. I-11). The value determined for the  $kT = 25$  keV neutron capture cross section of  $^{62}\text{Ni}$  is  $22.6 \pm 2.4$  mb. Results of stellar-nucleosynthesis calculations show that the weak component from  $s$ -process in massive stars is sensitive to this cross section.

\*Hebrew University, Jerusalem, Israel, †Forschungszentrum Karlsruhe Institute für Kernphysik, Karlsruhe, Germany, ‡Los Alamos National Laboratory, Livermore, CA, USA, §Soreq NRC, Yavne, Isr

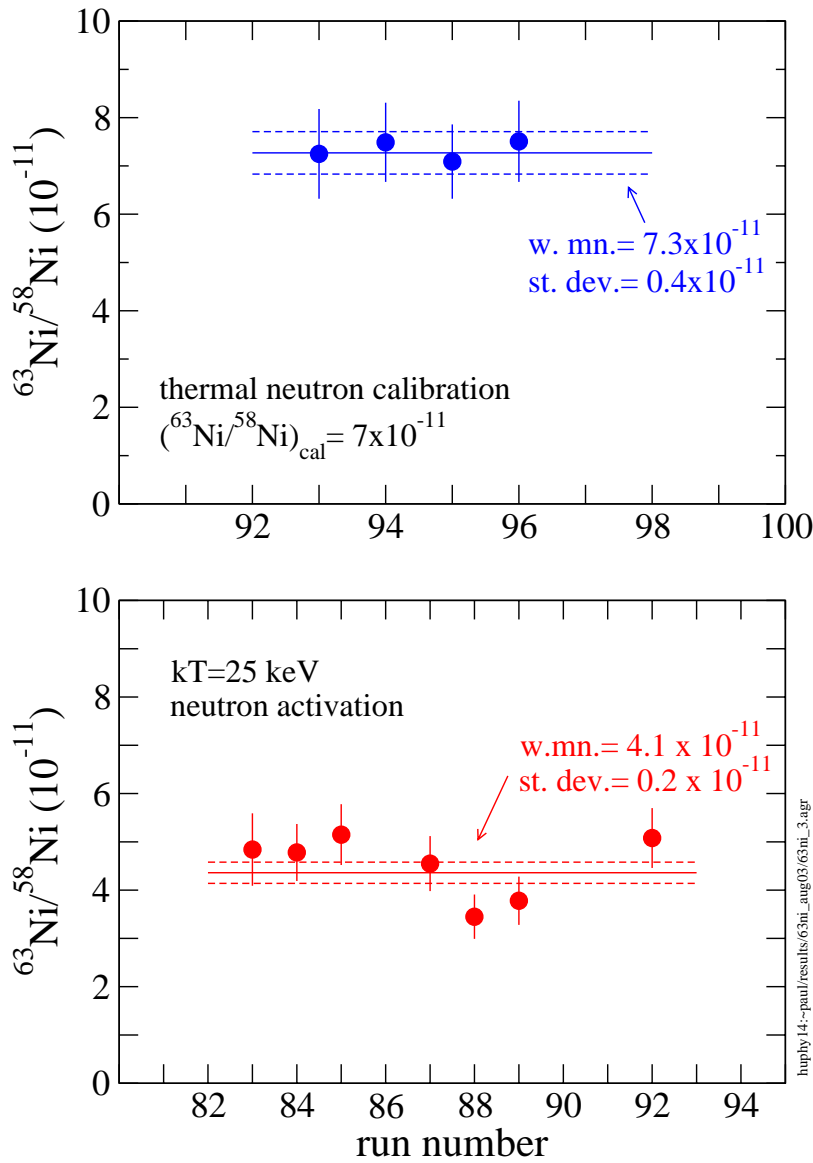


Fig. I-11. Repeat measurements of the isotopic abundance of  $^{63}\text{Ni}$  in the thermal-neutron activated sample (top) and the 25 keV-neutron activated sample (bottom). w.mn. is the weighted mean and st. dev. is the standard deviation.



### a.9 Absolute Intensities of $^{182}\text{Hf}$ Gamma Rays (I. Ahmad, J. P. Greene, E. F. Moore, W. Kutschera,\* and C. Vockenhuber\*)

The nuclide  $^{182}\text{Hf}$  was first produced by the neutron irradiation of natural Hf and enriched  $^{180}\text{Hf}$  targets in the Materials Testing Reactor at Idaho Falls. The Hf was chemically purified after  $^{175}\text{Hf}$  and  $^{181}\text{Hf}$  had substantially decayed and the new isotope  $^{182}\text{Hf}$  was identified by mass spectrometry and its half-life was determined as  $(9 \pm 2) \times 10^6$  y.<sup>1</sup>

In order to study the level structure of  $^{182}\text{Ta}$ , larger quantities of  $^{182}\text{Hf}$  were produced by Helmer *et al.*<sup>2</sup> Gamma-ray spectra of  $^{182}\text{Hf}$  were measured with a Ge detector. These studies showed that  $^{182}\text{Hf}$  decays by  $\beta^-$  particle emission and all strength goes to a single state at 270.4 keV in  $^{182}\text{Ta}$  which decays by 270.405-, 172.54-, and 156.09-keV gamma rays. After two years, the daughter  $^{182}\text{Ta}$  ( $T_{1/2} = 114.43$  d) reached secular equilibrium and its gamma rays were used to determine the absolute intensities of  $^{182}\text{Hf}$   $\gamma$  rays. A value of  $(80 \pm 5)\%$  per  $\beta^-$  decay was found for the intensity of the 270.4 keV gamma ray.

Currently there is interest in the half-life of  $^{182}\text{Hf}$  because the composition of  $^{182}\text{Hf}$ - $^{182}\text{W}$  samples can be used as a chronometer for early solar system evolution.<sup>3,4</sup> One component in the determination of the  $^{182}\text{Hf}$  half-life is the branching ratio of the 270.4 keV gamma ray. The large uncertainty in the intensity

of the 270.4 keV gamma ray measured by Helmer *et al.*<sup>2</sup> comes from the uncertainty in the intensity of the  $^{182}\text{Ta}$  gamma ray that was used as standard. Because the uncertainties in  $^{182}\text{Ta}$  gamma-ray intensities improved since the previous measurement and the sources used by Helmer *et al.* were available to us, we undertook the measurement of  $^{182}\text{Hf}$  gamma-ray intensities.

We measured the gamma-ray spectra of a  $^{182}\text{Hf}$  sample with a 25% Ge detector and also with a high-resolution 2 cm  $\times$  10 mm low-energy-photon spectrometer (LEPS). Spectra were measured by placing the source at large source-to-detector distances in order to reduce losses in the peak areas due to summing. A spectrum measured with a 25% Ge detector is shown in Fig. I-12. We determined the absolute intensity of the 270.4-keV gamma ray with respect to the intensity of the 222.1-keV gamma ray of  $^{182}\text{Ta}$ . The absolute intensity of the 222.1-keV gamma ray was previously measured<sup>5</sup> as  $(7.48 \pm 0.03)\%$  per  $^{182}\text{Ta}$   $\beta^-$ -decay. Using the above intensity of the 222.1 keV  $^{182}\text{Ta}$  gamma ray, the absolute intensity of the 270.4 keV gamma ray was found to be  $(79.0 \pm 0.8)\%$  per  $^{182}\text{Hf}$   $\beta^-$  decay. The results of this study were published.<sup>6</sup>

\*University of Vienna, Austria.

<sup>1</sup>J. Wing, B. A. Swartz, and J. R. Huizenga, Phys. Rev. **123**, 1354 (1961).

<sup>2</sup>R. G. Helmer, R. C. Greenwood, and C. W. Reich, Nucl. Phys. **A168**, 449 (1971).

<sup>3</sup>A. N. Halliday, Earth Planet. Sci. Lett. **176**, 17 (2000).

<sup>4</sup>A. G. W. Cameron, Nature **418**, 924 (2002).

<sup>5</sup>H. Miyahara, H. Nagata, T. Furusawa, N. Murakami, C. Mori, N. Takeuchi, and T. Genka, Appl. Radiat. Isot. **49**, 1383 (1998).

<sup>6</sup>I. Ahmad et al, Phys. Rev. C **70**, 047301 (2004).

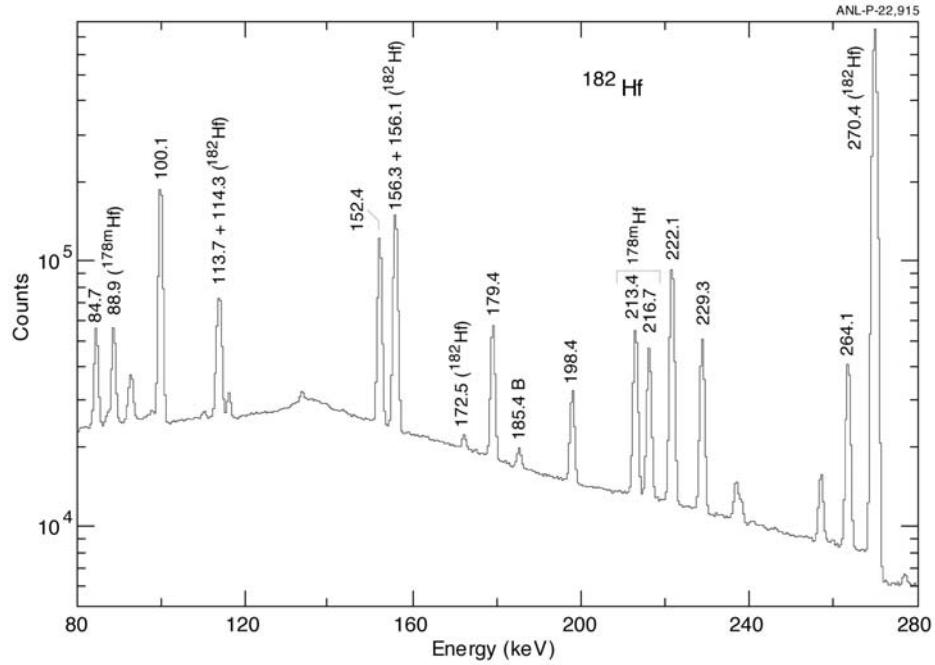


Fig. I-12. The gamma-ray spectrum of an 11-nCi  $^{182}\text{Hf}$  source measured with a 25% Ge spectrometer. In addition to  $^{182}\text{Hf}$  lines, the spectrum contains gamma rays from the daughter  $^{182}\text{Ta}$  and 31-y  $^{178m}\text{Hf}$ . B denotes background peaks.